Designing an operational C-band radar to realise the benefits of dual-polarization

T Darlington, M R A Edwards, V A Lissaman, R Riley, J Sugier,
M Kitchen, D Adams, R Cox, N Freeman, K Norman, R O'Boyle,
C Sloan, M Smees
Met Office, Exeter, EX1 3PB, UK

December 2016

Designing an operational C-band radar to realise the benefits of dual-polarization

By

T Darlington, M R A Edwards, V A Lissaman, R Riley, J Sugier, M Kitchen,

D Adams, R Cox, N Freeman, K Norman, R O'Boyle, C Sloan, M Smees

Met Office, Fitzroy Rd, Exeter, EX1 3PB, UK

Abstract

This paper describes the process whereby C-band radars in the UK National Network have been replaced by dual-polarization systems designed with an 'Open System Architecture'. That is, sub-systems from a range of sources have been integrated using industry-standard interfaces wherever possible. The approach was aimed at meeting the rather stringent performance criteria for successful exploitation of dual-polarization, whilst at the same time enabling future obsolescence to be managed more easily. The radar architecture is conventional, but with features that facilitate the ongoing development of additional radar parameters for measurement of atmospheric refractivity and radiances (passive emissions). Particular attention was paid to the specification of the antenna and radome, and as a result, the overall radar performance has met expectations with typical mode values of copolar correlation coefficient (ρ_{HV}) and linear depolarization ratio (LDR) of 0.997 and -34dB respectively within areas of light rain. It is shown that radar-to-radar variations of LDR in rain can be predicted based on the results of range testing each antenna prior to installation, a result that highlights the importance of testing individual antennas.

1. Introduction

Weather Radars are typically the most complex observing systems managed directly by National Meteorological Services (NMS's). They represent a significant capital investment, and maximising the benefits of this investment throughout their lifetime is a technical challenge for organisations where engineering tends to be a support function, rather than a core service. Many operational radar networks are either in the process of upgrading, or have recently upgraded, to dual-polarization systems. The potential benefits of dual–polarisation - in terms of improved accuracy of rainfall estimation, quality control and hydrometeor classification - are widely understood. However, recent work, notably by Hubbart et al (2010), has suggested that to fully realise these benefits, the demands upon the radar design, and particularly the antenna, are probably more stringent than previously thought. Of immediate concern is that the demands may be at the very limit of what can be achieved at an economic cost. The consequence of a sub-optimal implementation is a devaluation of the benefits, probably for the whole lifetime of the radar systems. Despite these concerns, there seems to be little available published information on how operational radar can be practically specified or designed to meet the performance criteria and achieve the advertised benefits of dual-polarization. The main purpose to the present paper is to try and fill this gap, at least for C-band systems.

Of course, any operational radar has simultaneously to meet many criteria, all of which influence the design. Perhaps one of the most important is the ability to manage obsolescence issues easily; minimising the longer-term risks to

operational availability. In such complex systems, obsolescence issues arise relatively frequently. Electronic subsystems, especially those incorporating processors, are likely to become unsupportable within a few years of manufacture, and well before the mechanical and electro-mechanical radar sub-systems are life expired. A fundamental choice facing most NMS's is then whether to adopt a capital-intensive approach to obsolescence and replace the radar systems wholesale, as and when the first serious obsolescence issue becomes apparent; or alternatively to tackle obsolescence in the radar sub-systems as and when it arises, with or without the assistance of the original supplier or a third party. The latter approach comes with a requirement that the necessary technical and engineering skills are available to do the work, and that a detailed technical knowledge of the radar systems is maintained. Evidence of these two different strategies being adopted can be seen in weather radar networks around the world, with some NMSs already running their third or fourth generation of radars, whereas others continue to maintain refurbished first or second generation systems.

The radar design described here has also been influenced to some extent by historical factors, which need to be explained. By the year 2000, the weather radar network in the UK comprised 14 C-band radars – near identical Siemens – Plessey Systems type 45C manufactured over the period 1976 to 1993 (hereafter referred to as '45C' radars). Production ended c. 1999 with SPS, by then part of BaE systems, withdrawing from the weather radar business. The 45C having such a long production run enabled the Met Office to maintain an almost uniform network with associated economies of scale in terms of spares holdings, training

and development costs. A disadvantage of the long production run was that obsolescence issues were starting to emerge very soon after the later radars were being installed. At this time, there was no thought to wholesale replacement of relatively new radars, so out of necessity, a radar development team started to form within the Met Office. Over the next few years, this team of engineers successfully introduced a range of enhancements to the radar systems including digital receivers designed and built in-house (see Darlington et al, 2004). When there was a requirement to add additional radars to the UK network, this was achieved by buying redundant 45C radars second-hand from around the world; refurbishing them, and upgrading to the latest network standard. In all, five used radars were purchased this way and three operational radars added to the network. This procurement programme also helped to maintain spares holdings at a satisfactory level during a period when some spares were not readily available from any other source. Throughout this period, radar engineering skills were acquired – partly through necessity – so that when it was clear that the 'make-do-and-mend' policy was no longer sustainable, the in-house team was in a position to design and build new radars.

Such a radical step was not without financial and technical risk, and could only be justified if the outcome was a radar that fully met requirements and could deliver the promised benefits of dual-polarization. There seems to be no recent precedent for the design and build of complete weather radar systems by a service provider. However, there are several examples of major upgrades by NMSs, where a user-developed signal processor has been interfaced with off-

the-shelf or existing hardware, e.g. see, Parent et al (2001), Rodriguez et al (2006) and Lane et al (2007).

To reduce the technical risks to acceptable levels, it was decided to construct a preliminary ‘demonstration’ radar before the majority of the investment was committed. This step provided an opportunity not just to demonstrate the concept to the network stakeholders, but also to refine the design and to develop the facilities that would be required for series manufacture and assembly. At the time of writing, nine radars to the new design are in operational use (with seven more to be constructed and installed). This is a sufficient number to be able to adequately characterise the in-service performance and also to quantify any differences across the network.

The design objectives for the radar are listed in section 2, followed by a description of the various radar sub-systems. Key results from the evaluation of radar performance are given in Section 3. Finally some general comments, including lessons learnt, are provided in Section 4. More detail concerning aspects of the capability and applications may be found in related, referenced publications.

2. System design

a. Output specification

The top-level design objectives are listed below in approximate order of priority.

- Assured continuity of existing data and products in the long-term.
- Network running costs contained at or below the previous level.
- Acceptable system whole life costs and performance.
- Dual-polarization capability, including both differential reflectivity (Z_{dr}) and LDR moments.
- Measurements of absolute phase and radiance to support ongoing development of new radar techniques.
- Flexibility to support development of new radar products in the future, as requirements change and opportunities arise.
- Reduced environmental impact from radar operations.

Although all of the above have a bearing on the design of the systems, a comprehensive evaluation of the new radar design against all the criteria is beyond the scope of this paper. We focus here on the more scientific aspects of radar capability and performance.

b. System architecture

The basic architecture of the dual-polarization radar (Fig 1) is a simplified version of a previous proposal for upgrading 45C radars developed by Bebbington (1998), and is similar to that described by Alford et al (2002). In the SHV (Simultaneous Horizontal and Vertical) mode of operation, the transmitter power is split at a point above the azimuth and elevation axes of

rotation, with pulses in the vertical (V) and horizontal (H) polarizations being transmitted simultaneously. The receiver and signal processor are also located immediately behind the antenna with two channels processing signals in H and V polarizations separately. The radar can also be reconfigured to operate in 'LDR mode' by the operation of a 4-port waveguide switch. In this mode, the transmitter power is not split, with transmissions confined to H polarization. The receiver functions exactly as before – with the V channel then providing a measure of the degree of depolarization by targets within the radar field of view.

The practical advantage of this arrangement is that it avoids the complication of two waveguides having to pass through a rotating joint, and avoids the radar signals having to traverse long waveguide runs (with associated losses), before reaching the receiver. Two practical disadvantages are that the receiver is placed in a relatively harsh environment within the radome, and there is the difficulty and expense of the necessary high-speed data link between the signal processor and the base of the tower. The means by which these disadvantages have been overcome are described below.

Radar control, signal and data processing, and communications functions are performed by a PC (called 'Cyclops - DP') which also provides a user interface for use by engineers at the radar site. To try and minimise future obsolescence, the interfaces between the different radar sub-systems are based on industry-standard protocols as far as possible. Almost all the adopted hardware is available off-the-shelf, and the radar design

incorporates just one bespoke circuit board, necessitated by a post-design modification.

c. Pedestal

The specification for the pedestal, in terms of size and load bearing, was unchanged from the previous generation radars. Hence in order to minimise cost and carbon footprint, the decision was made to re-use the basic castings from the 45C pedestals. Across the network, a total of approximately 25t of alloy has been re-cycled. The pedestal was re-engineered with new drive and servo systems, with industry-standard Controller Area Network (CAN) bus protocol used for all control and feedback functions. The brushless AC elevation and azimuth drive motors have an internal resolver for speed control and drive through a maintenance-free epicyclic gearbox. Absolute positional information is fed from a data take-off gear attached to both azimuth and elevation axes to a 14 bit Synchronous Serial Interface (SSI). The SSI signal is communicated via the CAN bus. A new sub-frame was mounted on the antenna yolk, upon which the receiver, signal processor and dual-polarization waveguide unit (see Fig 2) are fixed.

The pedestal incorporates a large slip ring assembly produced by Schleifring[1] which, as well as providing power and analogue signal connections, incorporates a high-speed channel for a PCIe bus connection (maximum data rate 10GBps) between the signal processor located behind the antenna, and the system PC located in the equipment cabin at the base of the radar tower.

[1] Schleifring Systems Ltd, Newbury, Berkshire, UK

For most of this distance, the PCIe bus is carried over a fibre optic cable, but is converted back to electrical signals for passage through the sliprings, where contactless connection is achieved by capacitive-coupling between rotating and stationary parts. The waveguide from the transmitter passes through a void in the centre of the slipring assembly to a separate rotating joint. A second identical rotating joint is required to take the waveguide through the elevation axis. Electrical and fibre connections are maintained across the elevation axis by including an additional ~1m run of cable mounted within a flexible cable tray.

d. Transmitter

The requirement for the new radars to measure atmospheric refractivity requires an ability to track the absolute phase of ground clutter returns. It was thought that successful implementation of this technique required the transmitter to be very stable in frequency, but Nicol et al (2013) showed that the STALO frequency stability was the main constraint. Hence lower cost/lower stability co-axial magnetron transmitters could be used.

Most European National Meteorological Services (NMSs) operating single-polarization C-band radars have historically used magnetrons producing ~250kW peak power. For SHV dual-polarization systems, in order to fully compensate for the 3dB loss induced by the splitting of the power, the transmitter power could be increased to ~500kW. This approach would involve higher power ratings (and cost) of several other components including the rotary joints, power splitter, couplers, the circulators, TR cells etc. Rather

than accept these additional costs, it was decided to seek to recover the 3dB loss of sensitivity in the design of the receiver (see section 2f below, and also Vaisala (2011) for further discussion on this topic).

The selected 250kW transmitter is manufactured by CPI[2]. Key features of the transmitter are the solid state modulator and a flexible interface in which the radiated pulse train will exactly mimic an input trigger waveform. This offers the possibility in the future to implement complex transmission schemes using a single control input. Currently, a 2.0 μs pulse is used for almost all routine reflectivity measurements in combination with a 300Hz pulse repetition frequency (PRF) and 300m range gate length. A 0.5 μs pulse width and 1200+900Hz dual-PRF is used in separate Doppler scans with a 75m range gate. These Doppler scans are also used to produce higher resolution rainfall products over some urban areas within 100km range of the radars.

e. Antenna and radome

As mentioned in the introduction, the criticality of the antenna design to the overall performance was recognised at the start. The key design criteria for the dual polarisation antenna are listed in Table 1. The 45C radars had a 3.7m circular parabolic antenna manufactured by Precision Antennas Ltd[3]. Although not designed with the requirements of dual-polarization in mind, results from the original range tests of these antennas (performed immediately following manufacture) suggested that they may be capable of approaching the dual-

[2] Communications and Power Industries, Beverly Microwave Division, Beverly, Mass, USA
[3] Precision Antennas Ltd are no longer trading

polarization design specification, once equipped with a dual-polarization feed. Even so, to further reduce the risk of nugatory work, photogrammetric measurements were made around a circle near the rim of these dishes to check for distortion. Deviations from a single plane were typically no more than 4mm, even for antennas purchased second-hand and known to have been subjected to inexperienced handling. Accordingly, Q-Par Antennas[4] were commissioned to design and carry out modifications to these original dishes to support dual-polarization measurements. New Potter- type feedhorns were installed supported by four stays, in place of the original three. Each antenna was subsequently tested on the Funtington test range of QinetiQ[5] to confirm that the design specification had been achieved. This range testing revealed a considerable variation in performance (see section 4), with two of these upgraded antennas having to be rejected as outside specification. Surprisingly, there was little correlation between the level of distortion revealed by photogrammetry and performance on the range. The short-fall in the number of antennas then available for the network was made up by new-build antennas of the same size and similar design to the original. The new dishes were spun by Elite Antennas Ltd[6], using a spinning lathe obtained from Precision Antennas Ltd, and very likely to be the same machine used to produce at least some of the original dishes for the 45C radars. Photogrammetric tests of these new dishes revealed a similar level of geometric precision to the older dishes.

[4] Steatite Q-Par Antennas, Leominster, Hereford, UK
[5] QinetiQ Group PLC, Farnborough, Hants, UK
[6] Elite Antennas Ltd, Leominster, Hereford, UK

In tests of two types of segmented panel radomes, Sugier et al (2007) found azimuthal variations in Z_{dr} and ϕ_{dp} due to differential transmission effects connected with the vertical seams in the radome construction. The variations were comparable in magnitude with the observed meteorological variations in Z_{dr} and proved surprisingly difficult to compensate for (Tabary et al 2009). A high priority was therefore given to avoiding this source of degradation of the dual-polarization moments, and a stringent radome specification was prepared (Table 1). Acceptance testing of the new radomes against this specification was judged to be too difficult and expensive. Instead, a cautious approach to procurement was adopted, whereby the first units to be delivered were subject to extensive in-service testing and evaluation before any additional units were ordered. In the event, the selected radomes ('Stealth® Radome' manufactured by AFC[7] and supplied through EEC[8]) proved satisfactory for dual-polarization use, and no azimuthal variations or other problems have been identified in the dual-polarization moments to date.

f. Receiver and signal processor

The receiver (Fig 3) is a dual-channel development of the previous single-channel receiver design for the 45C radars produced by the Met Office in collaboration with Pascal Electronics[9] (see Darlington et al, 2004). The design was refined to improve the sensitivity and to recover the 3dB loss resulting from the splitting of the transmitter power in Z_{dr} mode (see Fig 2). The requirement was to achieve a dynamic range of >80dB and > 50dB level

[7] Antennas for Communication, Ocala, Fl, USA
[8] Enterprise Electronics Corporation, Enterprise, Al, USA
[9] Pascal Electronics Ltd, Ryde, IoW, UK

isolation between the two channels, so that these subsystems did not impose any limit on the minimum value of LDR that could be measured.

The H and V signals are first amplified by Low Noise Amplifiers (LNA) with a nominal gain of 18dB and a noise factor of ~1.2dB (this figure depends upon the exact model of LNA used in each radar). This noise factor is an improvement of nearly 2dB compared to the previous radar receiver. Other gains in receiver sensitivity arise from the elimination of rotating joints from the receiver path and generally shorter waveguide runs. Together, these changes compensate for the 3dB loss in transmitted power when running in SHV mode. Furthermore, in a post-design modification, the LNAs are now being located directly on the output of the circulators, which produces a further improvement in SNR of ~1dB.

The 45C radars operated with an Intermediate Frequency (IF) of 30MHz, relying on image-rejection mixers to reduce the possibility and impact of interference at the image frequency. So that some of the RF components from the 45C receivers could be reused, the 30MHz IF was retained. Unfortunately, recent years has seen the appearance at some radar sites of interference entering the IF at the image frequency. To counteract this, as a short-term measure, an RF filter is being incorporated in-line with the LNA at the worst affected sites. This filter has an insertion loss of 0.5dB, so if the problem persists in the longer-term, a better mitigation might be to redesign the receiver with a higher IF.

Temperatures encountered within the radar radomes have not been systematically recorded, but probably extend over a range from ~ 0 to ~40degC. To avoid excessive heat build up in the receiver unit itself, it is ventilated by a thermostatically controlled fan, but neither the air in the radome or the air entering the receiver unit is cooled. The lack of a cooling system not only saves power and weight, but avoids adding a further source of heat within the radome. It does of course require that the receiver and signal processor are designed to tolerate a much higher range of temperatures, and these sub-systems were subjected to testing in an environmental chamber for both survivability and stability (see section 3b below). To avoid any possibility of condensation occurring within the receiver enclosure, it is also protected by a hydrostat which also activates the forced ventilation as required.

The signal processor is based on a single PCIe board produced by Pentek Inc[10], and is based upon a Field Programmable Gate Array (FPGA) module, with sub-modules providing multiple digital and analogue input and output channels (see Fig 4). The board is separated by up to 30m from its host PC, located in the equipment cabin at the base of the radar tower. The PCIe bus linking the two is carried on a fibre-optic cable, except for a short distance where it passes through the slipring assembly (see 2c above). Time synchronisation of the sampling of the two receiver channels is achieved by controlling the analogue-to-digital convertors (ADC) by an external

[10] Pentek Inc., Upper Saddle River, NJ, USA

programmable clock. The selected clock has an RMS jitter of <1ps and drives the ADC with a delay of <350ps.

The software (Fig 5) is a multi-threaded C++ program for scheduling radar scans, monitoring of the Automatic Frequency Control (AFC) function, processing I and Q data, product generation, and status monitoring. A volume scan task starts when the necessary conditions have been met within the Scheduler. The details of each scan making up the volume are then passed to the Radar object for it to configure the hardware appropriately. The radar object sets the rotation rate, elevation and sampling requirements for data acquisition, and then informs the Scheduler that it is ready. The specifications of the products to be generated from the volume data are passed to the Processing thread. The Processing thread then obtains the I and Q values from each pulse; phase corrects them and then calculates the average Doppler moments and dual-polarization parameters for 1 degree sectors (approximately matching the antenna beam width); then passes on this processed ray data into the product data stores where it can be operated upon to provide any additional averaging or other processing. When the product data store is full (i.e. the product is complete), the file is transferred to disk and the Scheduler informed. If no more products exist in the Processing thread, the Scheduler will move onto the next scan until the whole volume is complete. In a separate thread, the AFC processor is responsible for reading raw samples of the transmit pulse at IF, forming an estimate of the IF and generating requests for the Radar object to update the STALO or NCO in order to match the transmit frequency. As the STALO has a digital interface,

which controls the multiplication or division factor in phase locked loops to generate the STALO frequency, it is possible to measure the transmitter frequency as the sum of the STALO demand frequency and the current measurement of the IF.

In addition there are utility programmes running on the host PC that provide a basic local data display; enable manual control of the radar (if necessary for fault diagnosis); and radar status monitoring and reporting.

g. Refractivity and radiance measurements

Given the scale of the investment in the new radars, and the ongoing costs associated with running a national weather radar network, it is important to try and maximise the benefit obtained by extracting as much information as possible from the systems. Fabry (1997 and 2001) showed that weather radars have the potential to provide two additional types of measurement: near surface refractivity, and radiances (measurement of passive emissions). The new radars have been designed from the start to provide the basic data necessary for these techniques.

Early work on the refractivity technique in the UK used the previous single-channel radar receiver and signal processor which adopted a method of IF frequency control for accurate tracking of phase changes over extended time periods (see Nicol et al, 2008). This design has been carried over into the new dual- channel receiver. The refractivity data have been shown to be of

potential value for assimilation into convective scale numerical models (see Nicol et al, 2013) and assimilation tests have begun using data from the new radars (Simonin and Nicol, 2015).

For radiometric measurements to form a useful constraint on attenuation corrections, the target must be for the brightness temperature measurements to be stable to within ~10K (Darlington, 2014). A Ranatech[11] calibrated noise source is connected via a cross-coupler to the waveguide unit. It generates an excess noise ratio of 35dB, reduced to 5dB through the coupler. From testing in an environmental chamber, the output noise power (and hence equivalent noise temperature) was found to vary by about 2% over a 50 C temperature range. Radiometric measurements are made only in long-pulse mode and at ranges beyond 300km (i.e. from 2ms following each transmitter pulse) and for a duration of 1.33ms, During this period, the noise sources injects a pulse of 6µs duration for calibration purposes. The signals obtained from within the duration of the noise pulse are of course averaged separately. Details of the radiometric performance and plans for exploitation of these data are given in Husnoo et al (2015).

h. System integration

The first production series radar was installed at Wardon Hill in Dorset, and this site was used for the majority of the testing and evaluation. The 45C radars continued to be reliable and meet availability targets right up to the time of their replacement. There was little pressure then to incur extra cost in

[11] Ranatech Instrument AB, Flöjelbergsgatan, Mölndal, Sweden

a rapid roll-out of the new radars across the network. A single installation team could achieve a replacement rate of about three units per year, and this rate of construction proved to be largely within the existing staff and infrastructure resources. The procurement of workshop space for component storage, radar assembly and 'factory' testing, was the only additional requirement. Many components were purchased in bulk near the start of the project, to achieve economies in the procurement and also to guard against changes in component specification and consequential adjustments in the design. The exception was the radome where, as mentioned above, the inability to perform a specific acceptance test suggested a staged approach to procurement.

For series production of the receivers and signal processors, a test rig was devised for bench testing (Fig 6) prior to radar assembly. Workshop testing of the complete radars (minus antenna) was also conducted before the radars were again dismantled prior to transport to site for installation. This pre-installation testing paid dividends in terms of radar downtime, with all of the nine radars installed so far being functional on the same day as switch-on.

3. Testing and performance evaluation

a. Antenna performance

Hubbert et al (2010) and Zrnic et al (2010) have modelled the performance of SHV radars and concluded that to avoid serious biases in $Z_{dr,}$ the level of cross-polar isolation should ideally be ~40dB or better With this in mind, each modified and new dual-polarisation antenna was subjected to extensive

testing on an antenna range. A summary of the test results is given in Table 2, revealing a surprising level of unit-to-unit variability, even between antennas within the same batch. The antenna specification in Table 1 proved to be not quite achievable, and the decision was made to relax the requirements for sidelobe levels. The other criteria resulted in a ~25% antenna failure rate, which carried a significant cost penalty. This cost was accepted to avoid variable performance of dual-polarization algorithms and product quality across the radar network. A worst-case outcome would be that data processing algorithms would have to be tailored to individual radars, leading to higher software development and maintenance costs, and even difficulties in data interpretation by users. The rigorous approach to antenna testing paid dividends, in that when the radars were finally installed and tested, the quality of the dual-polarization moments was found to be excellent overall. The variations in antenna performance that are evident should have minimal practical impact on the performance, at least using the present generation of processing algorithms (see section 3c below).

b. Receiver and signal processor performance

The test harness shown in Fig 6 was used to measure the uncertainty in the Doppler radial wind measurements for a sample receiver. The results (Fig 7) showed that bias errors were confined to $<3 cms^{-1}$, which can be neglected when compared to typical observed spectral widths. The measured power response of the two receiver channels is shown in Fig 8. The response is approximately linear over a range >80dB with a minimum detectable signal of

<-125dBm. The isolation between the two channels is >65dB which is more than adequate to ensure that the receiver and signal processing subsystems do not present any limitation on the measurement of LDR (see section 4c below). With the receiver situated in an environmental chamber, repeated calibrations were performed at temperatures over the range 0-50degC. These showed variations of <1dB in each channel and ~0.3dB in Z_{dr} over the full temperature range. The variation in Z_{dr} was reduced to <0.1dB over a reduced range 0-25 degC. The uncertainty in Z_{dr} measurements should be confined to <0.2dB for rainfall measurement purposes (see e.g. Illingworth, 2004). For this reason, routine radar operation incorporates a 'zenith scan' performed every 10 minutes within the radar schedule (see e.g. Gorgucci et al 1999). Results from these scans form the basis of a dynamic correction (see below). Emissions from the sun can also be used for the same purpose (Gabella et al, 2014) and have the advantage that the measurements do not rely on the presence of rain. Variations in the receiver thermal noise also made calibration of the radiometric measurements more difficult. Although there is a marked diurnal variation in the noise level, the correlation with the receiver temperature is not simple, because of a significant thermal lag. The baseline noise level has therefore to be continuously monitored using precipitation free rays and subtracted from measured radiances in order to isolate emissions from the atmosphere (see Husnoo et al, 2015).

c. Radar performance in operation

Vaisala (2010) advocated the adoption of two key metrics to characterize the performance of dual-polarization radars. These are the mode values of ρ_{HV} and LDR measured within areas of widespread rain. A feature of these metrics is that they are readily measured from the standard 'in-service' system output, depending only on the selection of appropriate meteorological conditions, rather than requiring any special test equipment or environment. Fig 9 shows frequency distributions for a) ρ_{HV} and b) LDR recorded in areas of non-attenuating rainfall for each of the new radars, ρ_{HV} is a measure of the degree of overlap between the sample volumes in the different polarizations, and represents a limitation on the use of the K_{dp} parameter for improving rainfall rate estimates (Zrnić and Ryzhkov, 1996). LDR in light rain is another measure of the cross polar isolation, which represents a limitation on the use of Z_{dr} to improve rainfall estimates. There was no significant correlation evident between the mode values of these two quantities (Table 3). In contrast, there is a clear correlation between the antenna cross-polar isolation measured on the test range and both mode and min LDR measured in rainfall (Fig 10). A least squares fit to the data with slope constrained to be unity suggests that mode LDR can be predicted for any radar with a residual uncertainty of ~1dB, prior to radar assembly and installation. The strength of this correlation provides important reassurances concerning the radar systems themselves.

- As the cross-polar isolation as measured on the test range is a reliable predictor of in-service performance, decisions to accept or

reject antennas on the basis of the range tests alone were almost certainly correct.

- The level of cross-polar isolation is evidently dominated by the antenna performance, confirming that there are no problems of isolation elsewhere within the radar system.
- Neither transport of the antenna, nor repeated dismantling and reassembly of the support struts for the feed, seems to have impacted antenna performance.
- The lowest observed values of minimum and mode LDR in Fig 10 lie close to the trend line, with no evidence that some limiting value of LDR is being approached.

The close agreement in magnitude between the range measurements of cross-polar isolation and the minimum values observed in rain (Fig 10) may be just fortuitous. The measurements on the range are 'one way' – with de-polarization occurring upon reception only, whereas in the measurement of LDR, depolarization will occur on both transmit and receive. All other things being equal then, the expectation would be that the range measurements would exhibit higher levels of isolation. Approximately half of the radars installed so far have a minimum observed LDR at or below -40dB, which is the minimum level of cross-polar isolation recommended by Hubbert et al, 2010. Assuming the distribution of LDR around the peak is approximately Gaussian, then the uncertainty in LDR, $\sigma_{LDR,}$ may be estimated from the width of the distribution at a relative frequency of 0.5. This gives values of σ_{LDR} in the range 1.4 - 2.7dB, which should be $\sqrt{2}$ times $\sigma_{Z,}$ the uncertainty in the

measurement of Z. For integrations over ~35 radar pulses, and a normalised spectral width of ~0.17, as here, Doviak and Zrnic (1992) Fig 6.2 predicts a value of σ_Z =0.9dB and hence σ_{LDR} ~1.3dB, which is at the bottom end of the observed range. The causes of the radar-to-radar variation in σ_{LDR} evident in Fig 10b are unknown, and this may merit further study.

Temporal variations in the Z_{DR} offset, revealed by measurements at zenith, are shown in Fig 11. Fig 11(a) illustrates a period of ~ 1 day with high stability where variations in the offset varied by less than 0.1dB whereas 11(b) represents the typical; 'worst case' day for the same radar. To prevent such instability impacting products, frequent estimates of the offset are essential if errors in Z_{dr} are to be confined to <0.2dB.

4. Conclusions and lessons learned

A radical approach has been adopted for the replacement of the operational radars in the UK network. An Open System Architecture design, integrating off-the-shelf subsystems from a wide variety of sources, enabled the users to have full control over the component specification and hence the overall outcome in terms of radar capability. Although the scale and complexity of the engineering project was outside the normal scope of an operational service provider, historical factors meant that relatively few specialist services and expertise needed to be obtained externally.

Although the radar architecture is conventional, an excellent antenna and feed has delivered dual-polarization performance that exceeded expectations,

albeit with a surprising level of variability between similar units. The quality of the dual-polarisation parameters was predictable on the basis of range tests of each antenna. Although time consuming and expensive, the testing enabled sub-standard antennas to be rejected before installation. The cost of having to replace antennas post-installation would of course have been much higher. The variability in performance suggests that the antenna requirements may be at the limit as to what can be reproduced economically – echoing concerns raised by Hubbard et al (2010). If this is the case, then one way of achieving further gains in performance would be simply to adopt even more stringent antenna selection criteria, and accept an even higher rate of rejection.

The challenge presented by the hostile environment for the receiver was probably underestimated. Although the temperature stability of the basic reflectivity measurements is acceptable, Z_{dr}, being a difference measurement, exhibits more sensitivity which cannot be neglected. The offset value has to be monitored routinely using special zenith scans and a correction applied.

The use of an in-house signal processor has enabled the development of new radar capability to be maintained. Radar measurements of refractivity are now produced routinely with the expectation that assimilation trials will be successful and the data beneficial. The operational utilisation of radiance measurements within the radar data processing system is under development. It is hoped that these measurements can assist with quality control processes relating to partial beam blockage and provide improved

corrections for attenuation in rain. Here also, temperature sensitivities within the produce a diurnal variation in the noise floor; requiring continuous monitoring and corrections to be applied.

5. Acknowledgements

The authors would like to acknowledge advice and encouragement from Dr Robert Watson of Bath University, Mr Jon Eastment of the STFC, Rutherford-Appleton Laboratory and Prof Anthony Illingworth of Reading University. The radar project has involved a much larger group of people than can be included in the authorship of this paper. The contributions of the project managers: Nina Hartley, Pat Mackenzie, Chris Chadwick, and the engineering service teams managed by Richard O'Boyle are acknowledged in particular.

The Met Office is a customer of the component suppliers mentioned and referenced in this paper. No other commercial relationship exists, except in the case of Qinetiq PLC, to whom the Met Office also acts as a service provider.

6. References

Alford, J. L., J. J. Stagliano, and J. Helvin, 2002: Commercial simultaneous dual polarization radar. *Proc of the Sixth Symposium on Integrated Observing Systems.* 12-17 Jan 2002, Orlando, FL, USA.

Bebbington, D., 1998: Specification for Upgrading a Weather Radar to Polarization Diversity Capability. Met Office Contract Report. Copy available from the National Meteorological Library, Fitzroy Rd, Exeter, UK, EX1 3PB.

Darlington, T., M. Edwards, J. Sugier, and M. Kitchen, 2004: Opportunities presented by advanced off-the-shelf signal processing technology*. Proceedings of the Third European Conference on Radar Meteorology*. 6-19 Sept Visby, Island of Gotland, Sweden, p.291-295.

Darlington, T., 2014: Development, Evaluation and Applications of the Cyclops-DP Weather Radar Processing System. PhD Thesis, Dept of Electrical and Electronic Engineering, University of Bath.

Doviak, R. J. and D. S. Zrnić, 1992: Doppler Radar and Weather Observations. 2nd edition, Academic Press Inc. 562pp.

Fabry, F., C. Rush, I. Zawadski, and A.Kilambi, 1997: Extraction of near-surface index of refraction using radar phase measurements from ground

targets. *Antennas and Propagation Society International Symposium,* IEEE 1997 Digest Vol 4, p 2625-2628.

Fabry F., 2001: Using radars as radiometers: Promises and pitfalls. *Proc. 30th Int Conf on Radar Meteorology*, 19-24 July 2001, Munich, Germany, American Meteorological Society.

Gabella, M., T. M. Sartori, M. Boscacci, and U. Germann, 2015: Vertical and Horizontal Polarization Observations of Slowly Varying Solar Emissions from Operational Swiss Weather Radars, *Atmosphere,* **6**, p50-59.

Gorgucci, A., E. Scarchilli, and V. Chandrasaker, 1999: A procedure to calibrate mulit-parameter weather radar using properties of the rain medium. *IEEE Trans Geosci Remote Sens.,* **37**, p269-276.

Hubbert, J. C., S. M. Ellis, M. Dixon, and G. Meymaris, 2010: Modeling, Error Analysis, and Evaluation of Dual-Polarization Variables Obtained from Simultaneous Horizontal and Vertical Polarization Transmit Radar. Part I: Modeling and Antenna Errors*. J. Atmos. Oceanic Technol*., 27, 1583–1598.

Husnoo, N., T. Darlington, R. J. Thompson, and A. J. Illingworth, 2015: Combining constraints from emissions, reflectivity and differential phase for C-band attenuation correction. In preparation.

Illingworth A. J., 2004: Improved precipitation rates and data quality by using polarimetric measurements. In '*Weather radar'* (ed. P Meischner), Physics of Earth and Space Environments, Springer-Berlin Heidelberg. p130-166.

Lane, A., R. Atkinson, and R. Stringer, 2007: The Australian Weather Radar Network: Current and Future Challenges. *Proc 33rd Conference on Radar Meteorology*, 6-10 August 2007, Cairns, Australia. American Meteorological Society.

Nicol J., T. Darlington, A. J. Illingworth, K. Bartholemhew, M. Kitchen, and E. Delaygue, 2008: Operational testing of radar reflectivity retrieval for the UK radar network. *Proc 5th European Conf on Radar Meteorology and Hydrology.* 30 June- 4 July 2008, Helsinki, Finland.

Nicol, J., A. J. Illingworth, T. Darlington, and M. Kitchen, 2013: Quantifying errors due to frequency changes and target location uncertainty for radar refractivity retrievals. *J. Atmos. Ocean. Tech.*, **30**, 2006-2024.

Rodríguez, O. L., L. L. Fernández, R. A. Naranjo, A. Barreiras, A. A. Peña, M. Diez, W. Pozas, M. O. Aguiar, and J. L. Pérez**,** 2006: Cuban Weather Radar Network. Recent Advances and Future Plans. *Proc. 4th European Conf on Radar Meteorology and Hydrology* 18-22nd Sept 2006, Barcelona, Spain.

Parent, J., L. Perier, K. Do Khac and P. Roquain, 2001: CASTOR2, a new computer for the French radar network, *30th Int. Conf. on Radar Met*eorology

19-24th July 2001, Munich Germany, American Meteorological Society. p82-83.

Simonin, D. and J. Nicol, 2015: Quality Control of refractivity changes derived from weather radar. In preparation.

Sugier, J. R. J.Thompson, A. J. Illingworth, M. L. Segond, and P. Tabary, 2007: Correcting for radome interference effects on differential reflectivity measurements; implications for operational rainfall estimates. *Proc. 33rd Conference on Radar Meteorology*, 6-10 August 2007, Cairns, Australia. American Meteorological Society.

Tabary, P., A. A. Boumahmoud, B. Fradon, J. Parent-du-Châtelet, H. Andrieu, and A. J. Illingworth, 2009: Evaluation of two integrated techniques to estimate the rainfall rates from polarimetric radar measurements and extensive monitoring of azimuth-dependent Z_{dr} and phiDP biases. *Proceedings of the 34th Conference on Radar Meteorology*, Williamsburg, VA. USA. American Meteorological Society.

Vaisala, 2010: What is the Max RhoHV of Your Radar? What is the Min LDR of Your Radar? Vaisala 'White Paper', Vaisala Oy, Helsinki, Finland. Available for download from the Vaisala website at: http://www.vaisala.com/Vaisala%20Documents/White%20Papers/MET-What_Is_the_Max_RhHV_of_Your_Radar-white_paper-B211072EN-A-LoRes.pdf

Vaisala, 2011: With Vaisala Dual Polarization Enhanced Reflectivity - Radars See More! Vaisala 'White paper', Vaisala Oy, Helsinki, Finland. Available for download from the Vaisala website at: http://www.vaisala.com/Vaisala%20Documents/White%20Papers/MET-G-White%20Paper-Radars%20See%20More-B211164EN-A-LoRes.pdf

Zrnić D. S. and A. Ryzhkov, 1996: Advantages of Rain Measurements Using Specific Differential Phase. *J. Atmos. Oceanic Technol*., **13,** 454–464.

Zrnić, D., R. Doviak, G. Zhang, A. Ryzhkov, 2010: Bias in Differential Reflectivity due to Cross Coupling through the Radiation Patterns of Polarimetric Weather Radars. *J. Atmos. Oceanic Technol*., **27,** 1624-1637.

Tables

Table 1 Radar Design Aims

Radome	Cross polar degradation	<0.5dB
	Maximum transmission loss	0.1dB (dry) and 0.5dB (wet, at a rainrate of 20mm/h)
	Sidelobes	<0.5dB
Antenna	Shape	Parabolic
	Diameter	3.7 m
	Feed type	Potter feed
	Average gain	> 43 dB
	3dB beam width	< 1.1 deg
	Average side lobe, dB	<-30dB within ±10° and <-35deg outside ±10°.
	Cross-polar isolation	<-40dB
Transmitter	Wavelength, cm	5.3
	Peak power, kW	250
	PRF	300 long pulse, 900/1200 short pulse
	Pulse width, µs	2us long pulse, 0.5us short pulse
	Polarisation mode	H and V transmit and receive, or H transmit and H and V receive
Receiver	Noise figure	< 2.5 dBm
	Minimum detectable signal @ 1MHz	< -110 dBm
	Dynamic range	> 90 dB
	Maximum range	255 km long pulse, 120 km short pulse
	Minimum resolution	300 m long pulse, 75 m short pulse
Output	Measured parameters	Z_H, Z_V, Z_{dr}, ϕ_{dp}, ρ_{HV}, LDR, V, SQI, CPA, refractivity, radiance
	Mode ρ_{HV} in non-attenuating rain	> 0.997
	Mode LDR in non-attenuating rain	< -35 dB
	LDR system limit	- 42 dB

Table 2 Range testing of Antennas

Antenna serial number	*Radar site where currently installed*	*Manufacturer and approx year of manufacture*	*Half-power beam width (deg)[1]*	*Gain (dB)[2]*	*Average power in sidelobe (dB relative to peak)[3]*	*Average level of cross-polar isolation (dB)[3]*	*Pass/fail against specification*
5780	Wardon Hill	Precision 1998	1.1	43.6	-28.3	-40.04	pass
02246	Chenies	Precision 1983	1.1	44.0	-27.8	-38.96	pass
01401	Castor Bay	Precision 1986	1.1	45.0	-31.8	-37.44	pass
11623	Predannack	Elite 2011	1.1	43.8	-32.1	-41.62	pass
12018	Cobbacombe Cross	Elite 2011	1.1	44.0	-29.3	-38.54	pass
00778	Hameldon Hill	Precision 1976	1.1	44.5	-33.1	-38.25	pass
08082	Hill of Dudwick	Precision 1991	1.0	43.6	-30.8	-38.29	pass
04953	Ingham	Precision 1987	1.0	N/A	-30.7	-33.94	marginal pass
15993	Clee Hill	Elite 2013	1.1	43.9	-29.7	-39.87	pass
02637	-	Precision 1990	1.1	43.8	-30.7	-33.97	fail (cross-polar)
04954	-	Precision 1986	1.1	45.5	-31.8	-31.59	fail (cross-polar)
11624	-	Elite 2011	1.1	43.0	-31.5	-40.70	fail (gain)
	Thurnham	Andrew[4] 2002	untested				

[1]the half power beam width was measured in two orthogonal planes and in H and V polarizations (4 measurements in total)

[2]The gain is measured at a nominal 5.625GHz and is an average of measurements in H and V polarizations.

[3]The values are an average over 2 different planes for transmission (45, and 135 deg, relative to a reference azimuth on the dish) and reception (135 and 45 deg respectively). The test was conducted for transmission in both H and V polarizations, giving 4 values altogether. Transmission at 0 and 90 deg was excluded as these are the planes of the feed support struts.

[4] Andrew Corp, Orland Park, Il, USA.

Table 3 In-service Radar Performance

Radar site	*Radar number*	*Mode* ρ_{HV}	*Mode LDR*
Wardon Hill	11	0.9970	-36.0
Chenies	5	0.9975	-34.1
Castor Bay	7	0.9955	-33.0
Predannack	8	0.9975	-38.3
Cobbacombe Cross	16	0.9965	-34.5
Hameldon Hill	4	0.9985	-35.3
Hill of Dudwick	14	0.9965	-32.8
Ingham	9	0.9965	-31.3
Clee Hill	3	0.9955	-34.8
Average		*0.9975*	*-34.3*
Thurnham[1]		0.975	-24.1

Notes

1. The Thurnham radar antenna was not subjected to tests on a range prior to installation, and the data obtained in service suggests that this antenna has a serious defect. A new antenna will be installed once all the other new radars are installed and in service. Data for this antenna are not included in Figs 9 and 10.

List of Figure Captions

Fig 1 - Radar architecture overview. Components above the dashed line rotate in azimuth.

Fig 2. Schematic of waveguide unit located above the elevation Axis. The waveguide switch is shown set to the LDR mode of radar operation.

Fig 3. Block diagram of dual-channel receiver.

Fig 4. Block diagram of signal processor.

Fig 5. Schematic diagram of the signal processing software.

Fig 6. Test harness for radar receiver and signal processor.

Fig 7. Errors in velocity recorded using the test harness in Fig 6.

Fig 8. Results from calibration of the dual-channel receiver. a) signal injected in the H Channel and b) the V channel.

Fig 9. Frequency distributions of a) ρ_{HV} (transformed to a log scale to aid clarity) and b) LDR recorded in areas of widespread non-attenuating rain (measured reflectivity in the range 20-25dBZ) . Table 3 lists the peak values in each distribution.

Fig 10. The average cross-polar isolation measured on the test range compared to LDR recorded in non-attenuating rainfall (measured reflectivities in the range 20-25dBZ). The fitted lines are constrained and have a gradient of 1. Values of mode LDR are marked by the diamond symbols and fitted by the dashed line. The triangle symbols fitted by the dash-dot line denote the minimum observed LDR (defined here as being where the frequency distribution of LDR falls to 1% of the value at the peak). The values of the intercepts are -1dB for min LDR and 4.2dB for mode LDR.

Fig 11. Sample time series of Z_{dr} offset obtained from measurements at zenith in rain from the Predannack radar. a) shows typical ‘best case’ stability, and b) represents typical ‘worst case’. The

larger symbols are the mean values of Z_{dr} recorded during the scans, and the smaller symbols above and below show the standard deviation.

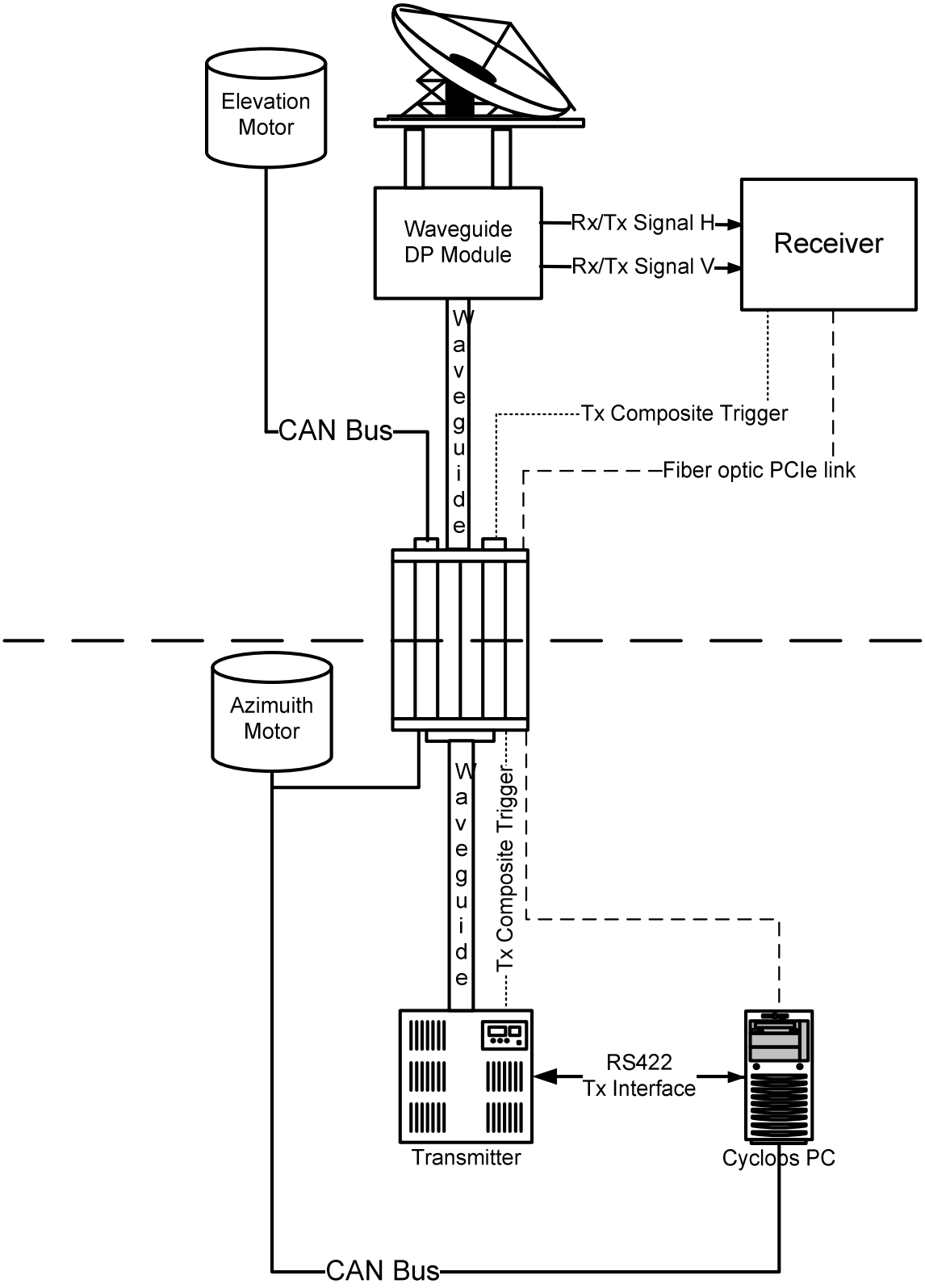

Fig 1. Radar architecture overview. Components above the dashed line rotate in azimuth..

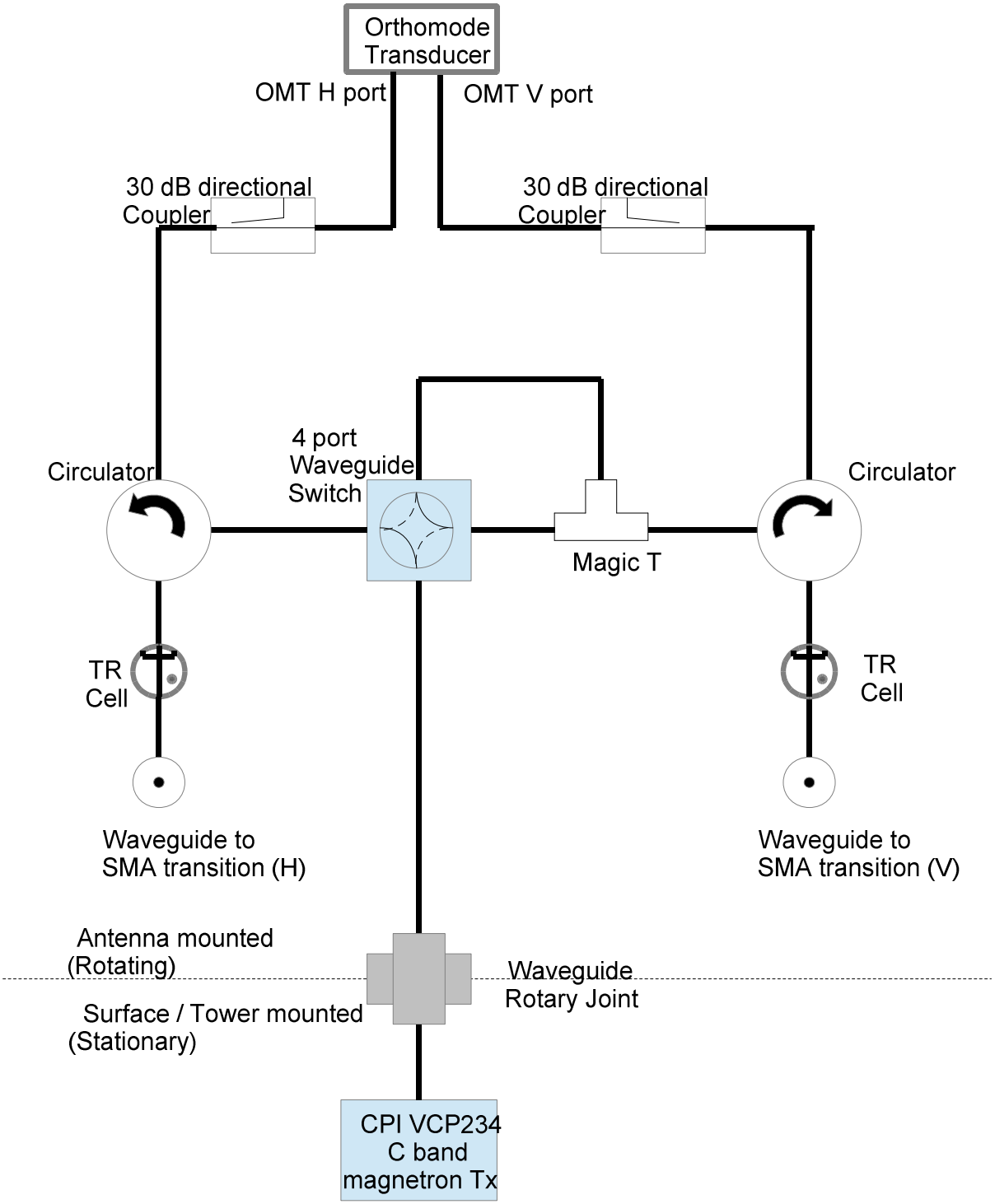

Fig 2. Schematic of waveguide unit located above the elevation axis. The waveguide switch is shown set to the LDR mode of radar operation.

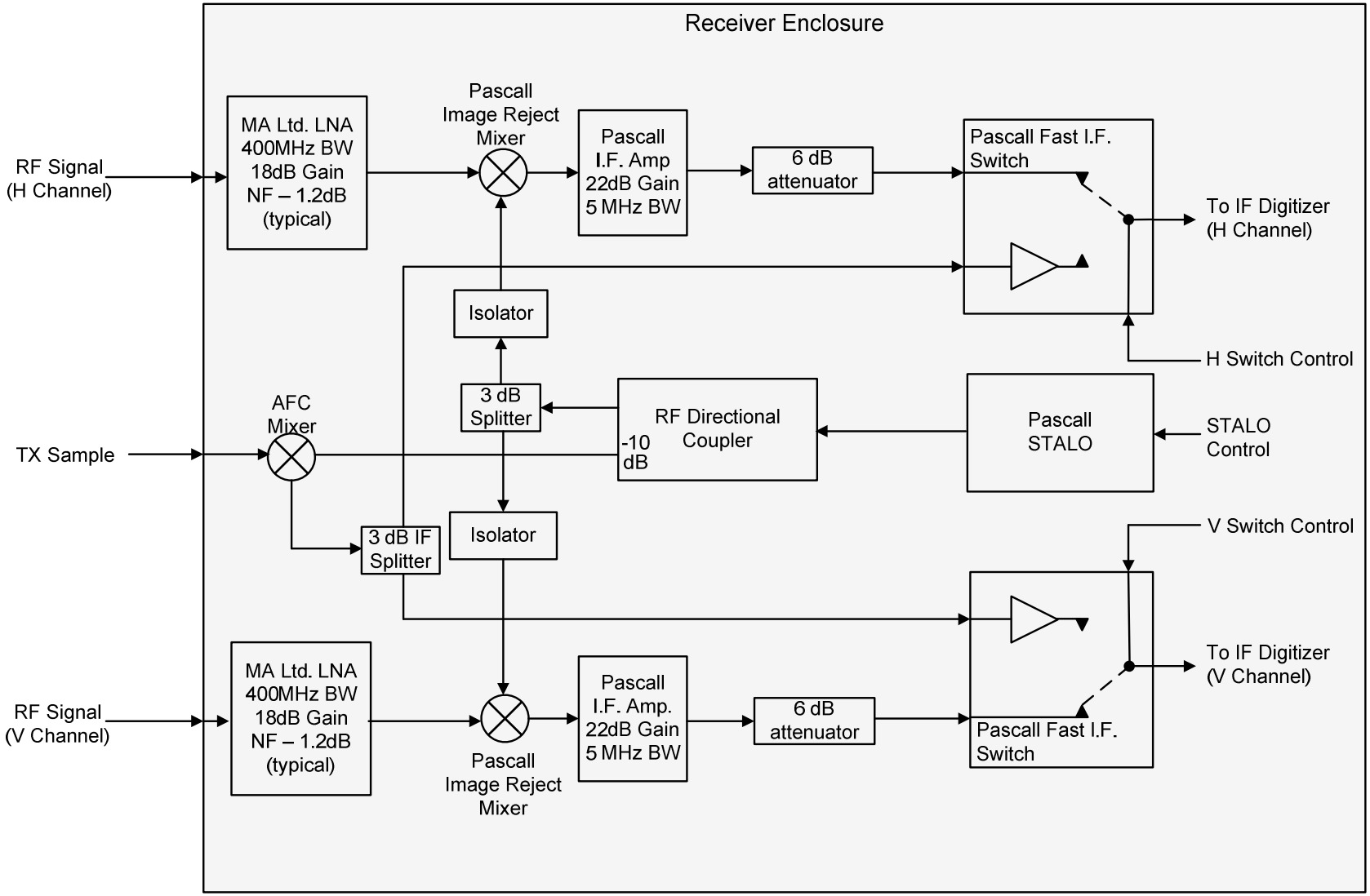

Fig 3. Block diagram of dual-channel receiver

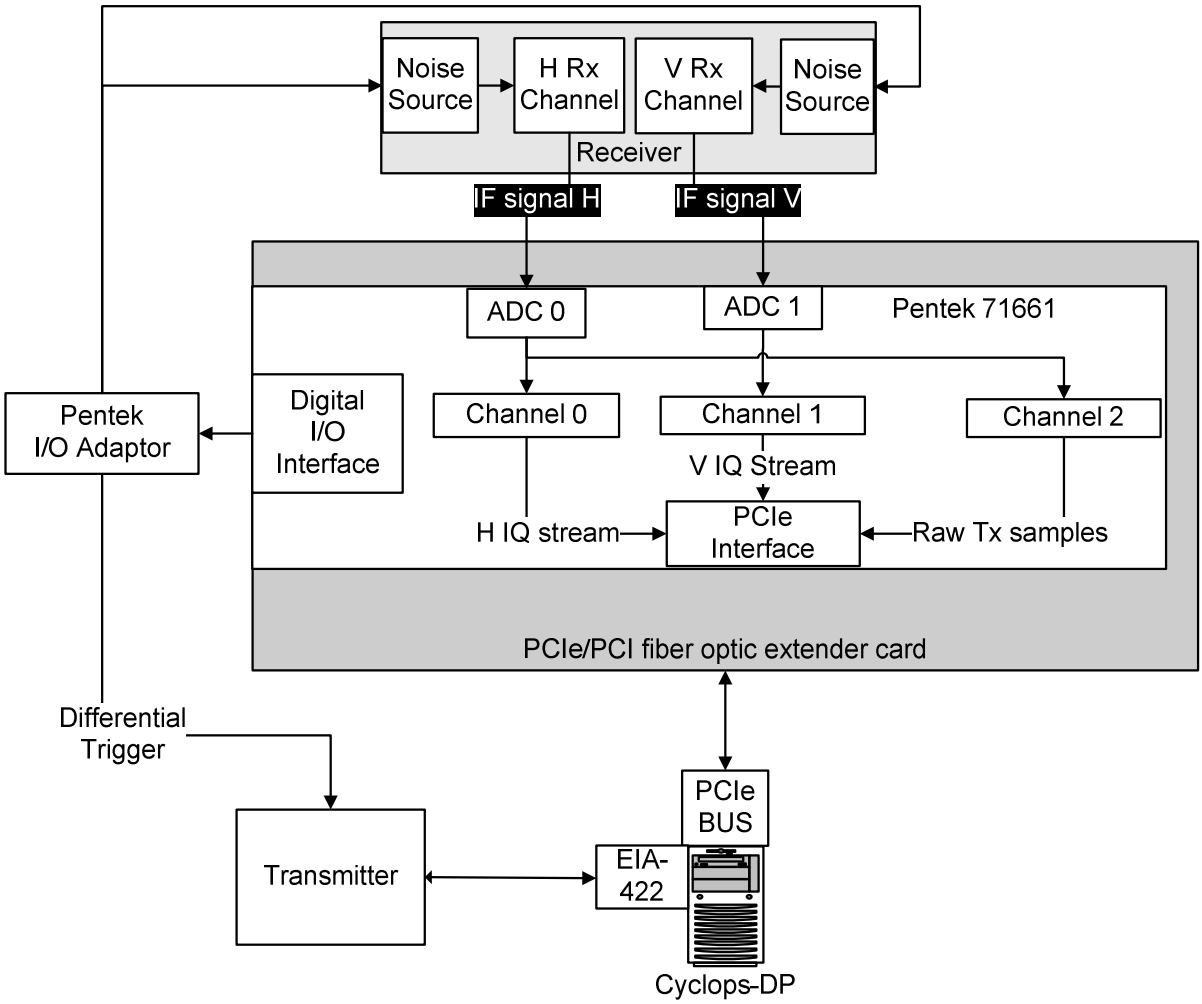

Fig 4. Block diagram of signal processor

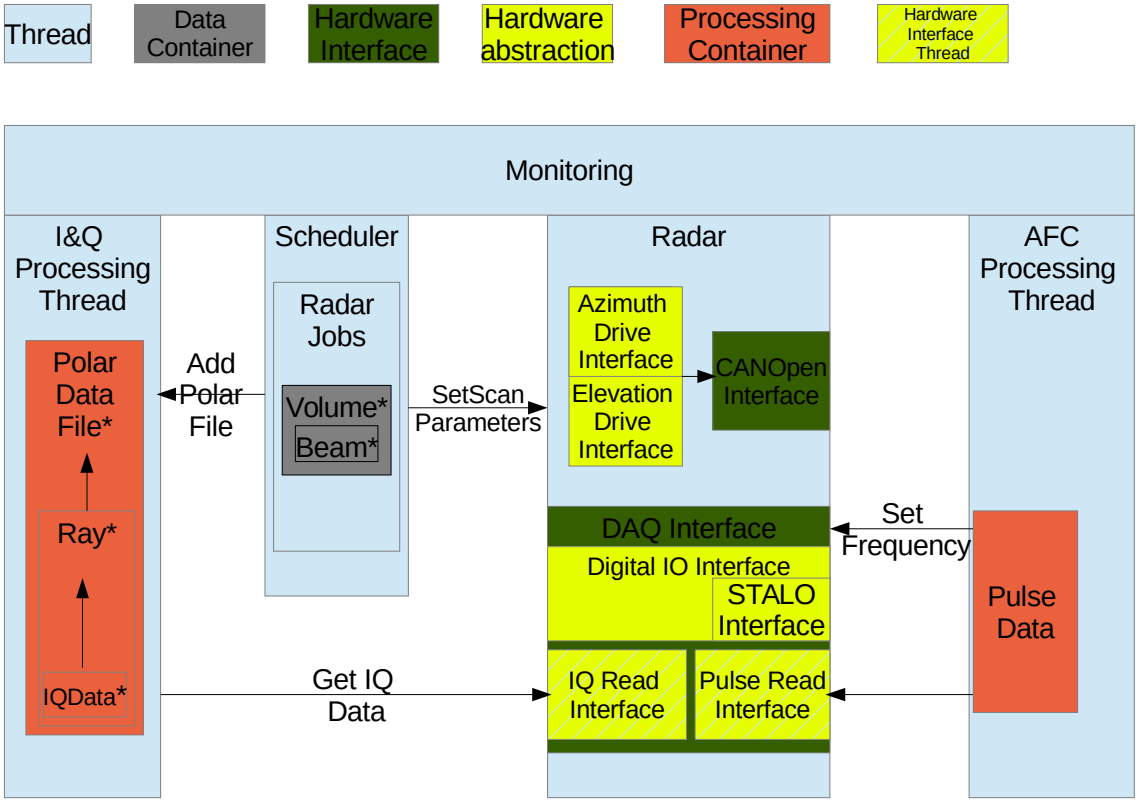

*multiple instances of these objects exist concurrently

Fig 5. Schematic diagram of the signal processing software

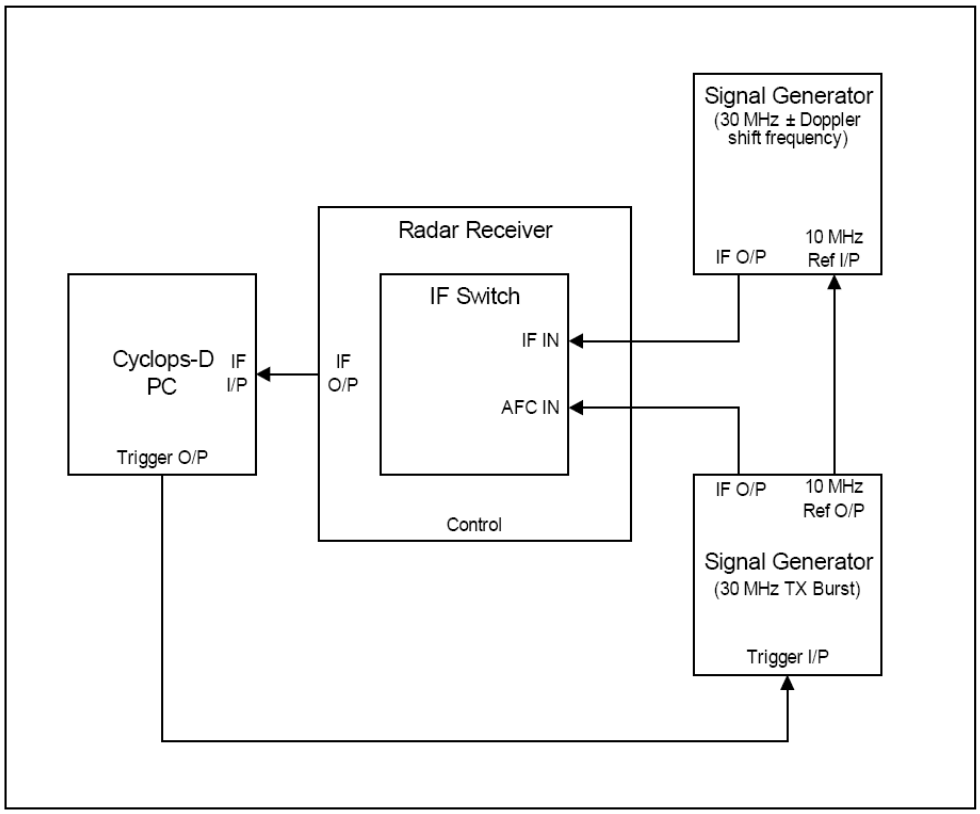

Fig 6. Test harness for the radar receiver and signal processor.

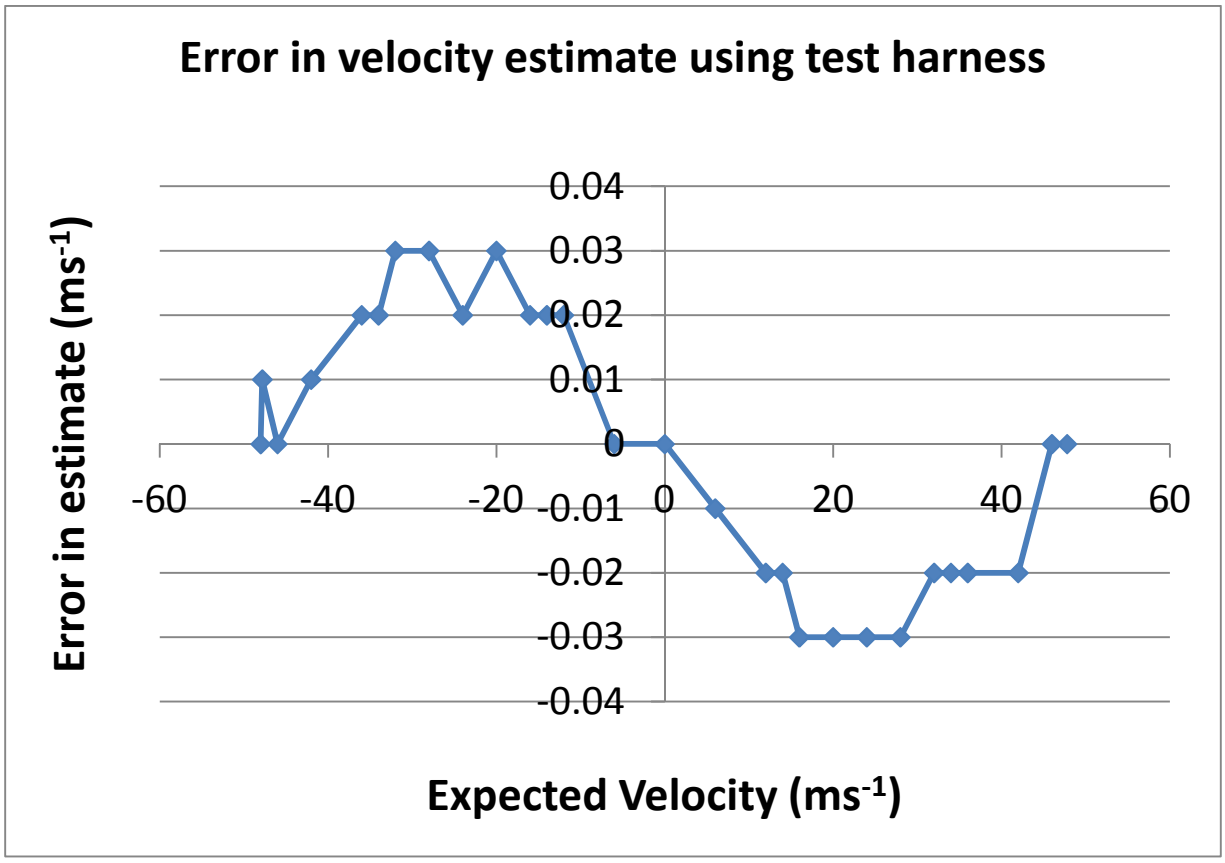

Fig 7. Errors in velocity recorded using the test harness in Fig 6.

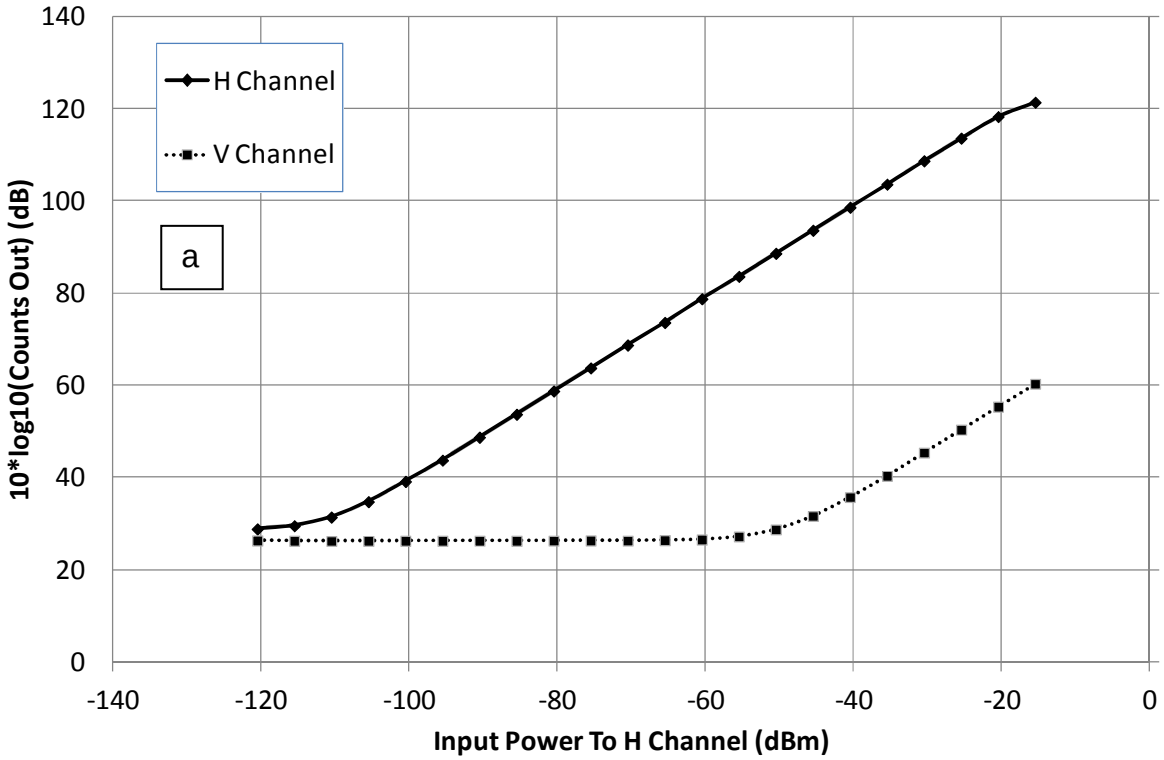

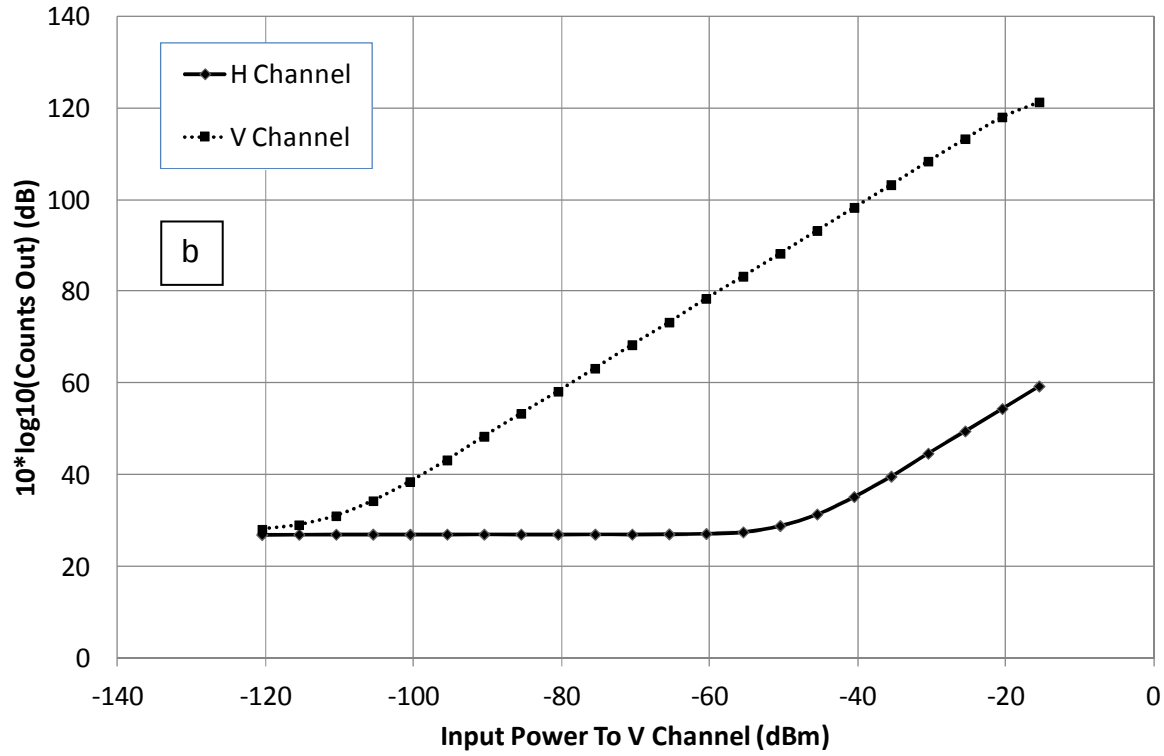

Fig 8. Results from calibration of the dual-channel receiver. a) signal injected in the H Channel and b) the V channel.

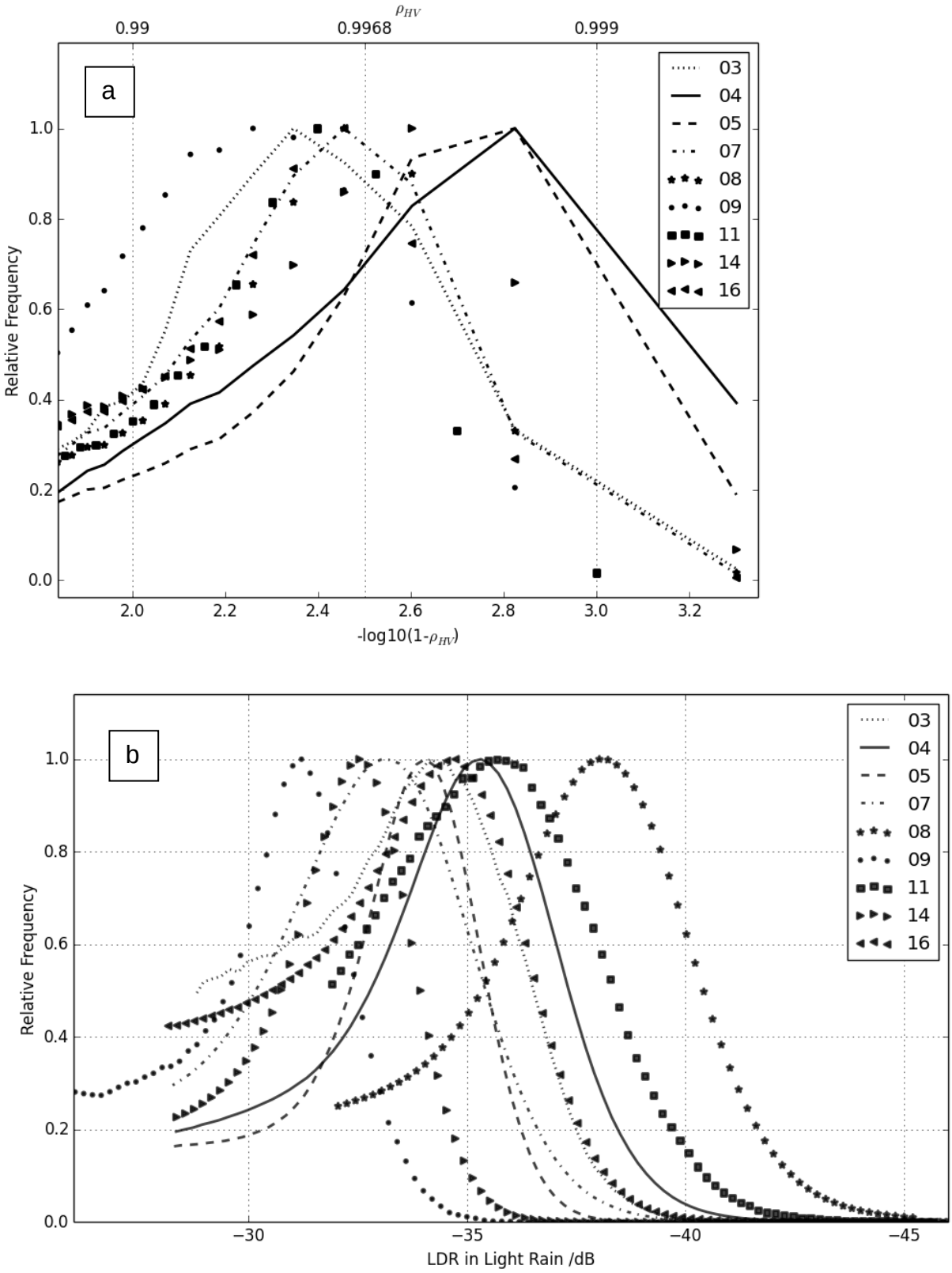

Fig 9. Frequency distributions of a) ρ_{HV} (transformed to a log scale to aid clarity) and b) LDR recorded in areas of widespread non-attenuating rain (measured reflectivity in the range 20-25dBZ) . Table 2 lists the peak values in each distribution.

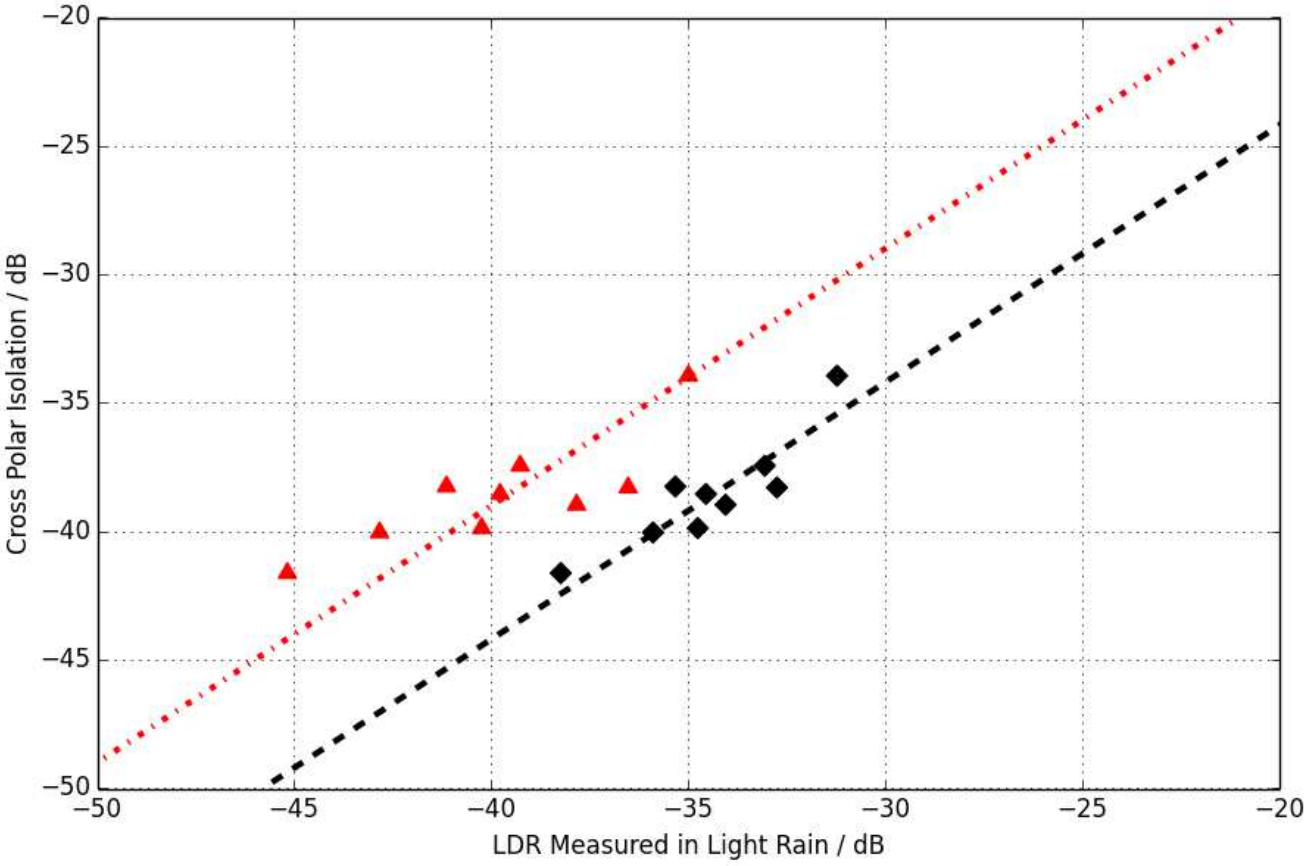

Fig 10. The average cross-polar isolation measured on the test range compared to LDR recorded in non-attenuating rainfall (measured reflectivities in the range 20-25dBZ). The fitted lines are constrained the have a gradient of unity. Values of mode LDR are marked by the diamonds and fitted by the dashed line. The triangles fitted by the dash-dot line denote the minimum observed LDR (defined here as being where the frequency distribution of LDR falls to 1% of the value at the peak). The values of the intercepts are -1dB for min LDR and 4.2dB for mode LDR .

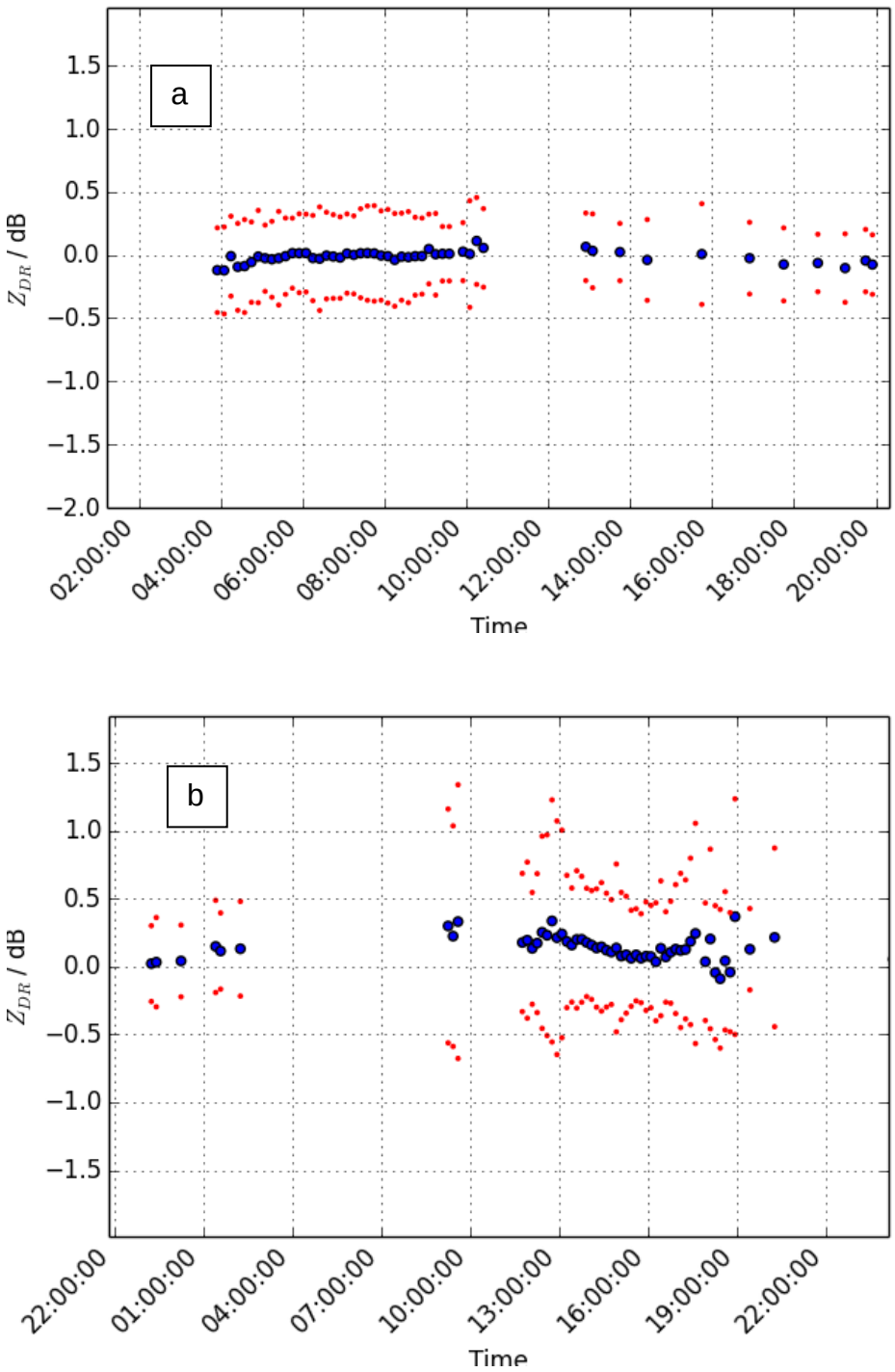

Fig 11. Sample time series of Z_{dr} offset obtained from measurements at zenith in rain from the Predannack radar. a) shows data from 26 January 2014 – an example of a day with high stability, and b) is from 25 May 2014, which is typical of the largest diurnal variations that have been observed. The larger symbols are the mean values of Z_{dr} recorded during the scans, and the smaller symbols above and below show the standard deviation.